

14.3

Investigation of the relief geometry of the membrane of human buccal epithelium cells using atomic force microscopy methods

© N.A. Torkhov, M.P. Evstigneev, A.A. Mosunov, V.A. Buchelnikova

Sevastopol State University, Sevastopol, Russia
E-mail: andrewmosunov@gmail.com

Received November 11, 2021

Revised January 17, 2022

Accepted February 1, 2022

The analysis of the shape of the Brownian relief of the surface of human buccal epithelium cells was carried out using the method of fractal geometry. The scaling coefficients η , ξ and the fractal dimension D_f were used to estimate their actual areas $S_{c(fact)}$ and linear characteristics l_f .

Keywords: atomic force microscopy, buccal epithelium, fractal number.

DOI: 10.21883/TPL.2022.04.53169.19074

The area of outer surfaces of cells plays a significant part in their homeostasis and in the processes of human immune system stimulation. It is well-known that the human immune system reacts not to the number, but to the total surface area of foreign particles and is activated when a certain threshold value, which is defined by the ratio of total surface area S_p of particles to surface area $S_{c(fact)}$ of a cell ($S_p/S_{c(fact)}$), is reached [1,2]. It is also known that functional pathological changes in the surface morphology of buccal epithelium cells are correlated well with homeostatic disruption indicators of the human body as a whole, thus providing an opportunity to perform rapid and fairly affordable evaluation of the overall condition of the body [3–7].

In addition, the current rapid development of biomechanical nanosystems implies integration of the human body with various biomechanical nanodevices; this requires the development of methods for examination of the mechanical properties of the human body at the cellular level. Specifically, the cell membrane surface largely shapes the possibilities of its mechanical fixation and movement in the medium or along an external surface, as well as the ability of foreign objects (e.g., zero-dimensional ones: quantum dots (molecules, fullerenes, etc.); one-dimensional ones: quantum filaments (complex organic molecules, quantum wires); two-dimensional and three-dimensional ones: flat and three-dimensional nano-objects) to attach to the cell surface and move along it [4]. In the general case, geometric parameters of the cell membrane relief are needed to characterize the mechanisms of interaction between it and various internal and external objects; their travel path, momentum and speed of motion; the mechanical work performed in the process; the energy dissipation; and the thermodynamic potentials. The study of such properties of cells is the basis for atomic and molecular nanoengineering (manipulation of nanoobjects, production of micro- and nanostructured devices) both on the surface of a cell and inside it.

Although evident progress has been made in research into the micromechanical properties of cell membranes [3,8–10], experimental data on the shape and geometry of the surface relief of buccal epithelium cell membranes are extremely scarce, and further study is needed. This is often attributable to the lack of proper approaches and methods of examination of surfaces of live biological objects at the cellular level.

Living human buccal epithelium cells obtained by liquid-based cytology were studied in air under normal conditions on an epitaxial Si{111} surface (Fig. 1, *a*; see also supplementary materials, Appendix A). The drying regime used in sample preparation was chosen so that a protective adsorption layer of a buffer solution with a thickness on the order of 100 nm remained on the cell surface. This layer prevented the cells from drying out and provided an opportunity to preserve their viability in air for no less than 2.5 h. This was confirmed by the dye exclusion method (trypan blue). After 2.5 h, most of the cells were resistant to the dye.

The surface relief of the cell membrane was measured using an NTEGRA SPECTRA atomic force microscope (AFM) and an HA_FM/W₂C cantilever in the contact scanning mode (with constant force $F_z = F_{const} \approx 20$ nN). This study was carried out at the „Molecular Structure of Matter“ common use center of the Sevastopol State University (see supplementary materials, Appendix B). The possibility of direct control over constant static pressing force F_{const} is an important feature of the contact method. Specifically, this allows one to work with adsorption layers of various thickness and nature. This approach combined the advantages of „dry“ [7] and „wet“ [11] scanning methods.

The parameters of surface relief of the cell membrane (actual area $S_{c(fact)}$ and length l_f of the section profile) were analyzed within the mathematical framework of fractal geometry by determining the values of scaling coefficients η , ξ and fractal dimension D_f ((see supplementary materials, Appendix C) [12]. The

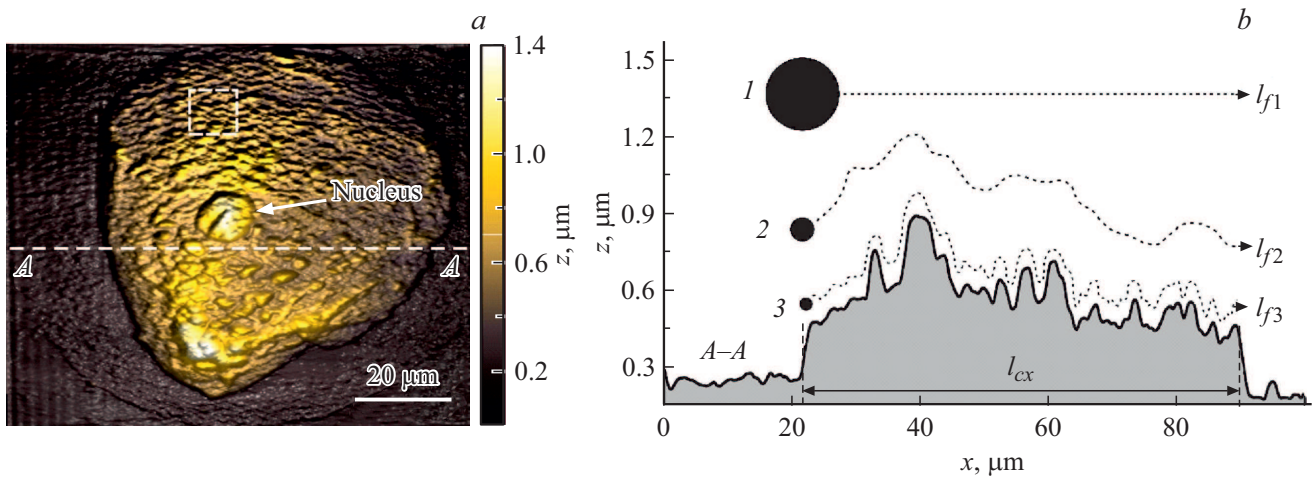


Figure 1. *a* — Half-tone 3D image of relief $h(x, y)$ of a region ($100 \times 100 \mu\text{m}$) of the epitaxial Si{111} surface with a living human buccal epithelium cell positioned on it. This image was obtained in the contact AFM scanning mode with a constant pressing force. *b* — Profile $h(x)$ of transverse relief section A–A with a schematic representation of the trajectories of motion of microparticles ($I - 5.00 \mu\text{m}$, $2 - 0.32 \mu\text{m}$) and nanoparticles ($3 - 100 \text{ nm}$).

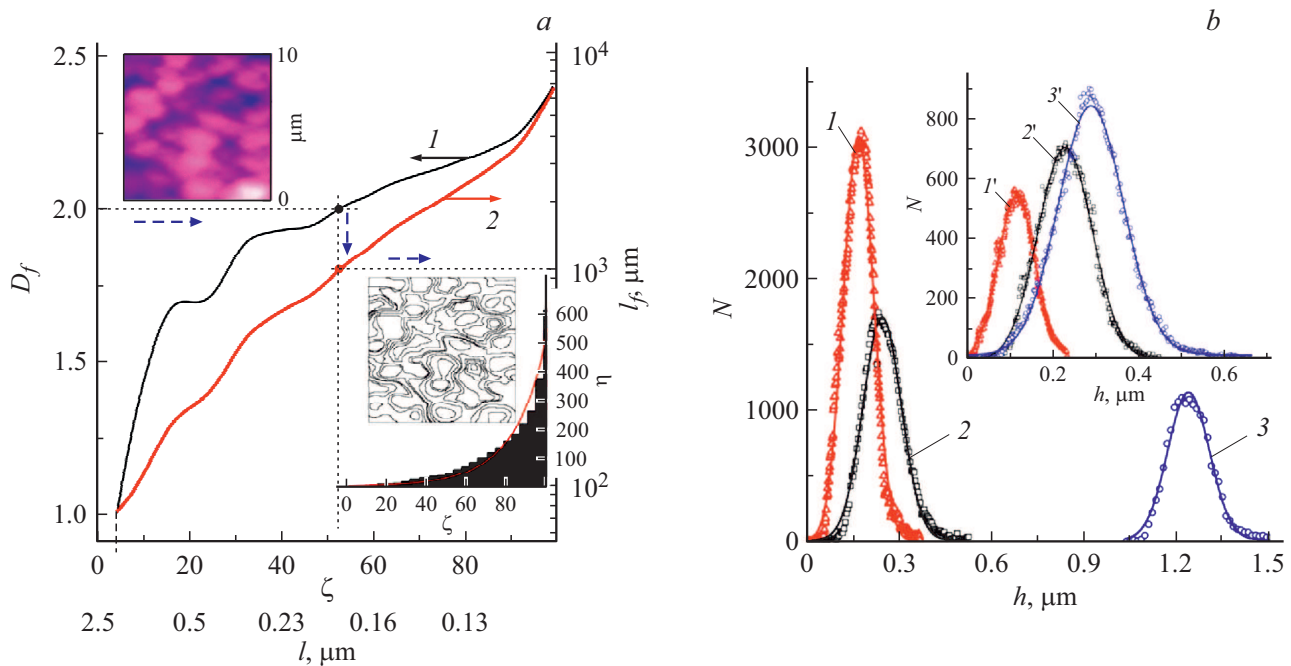


Figure 2. *a* — Dependences of fractal dimension D_f (I) and actual travel path length $l_f = l_f(D_f)$ (2) on scaling coefficient ξ . The corresponding values of l for the studied region are indicated below the ξ values. The topology of the studied region ($10 \times 10 \mu\text{m}$) is presented in the upper inset, and the lower inset shows its contour image with exponential approximation (solid curve) of the „devil's staircase" $\eta = 1.628 \exp(\xi/17.527)$. *b* — Typical histograms $N = N(h)$ of the distribution of irregularities within a square region of the surface of a membrane of a live human buccal epithelium cell for different measurement methods with a constant resolution of 256×256 pixels and different linear dimensions: $I - 5 \times 5 \mu\text{m}$, $2 - 10 \times 10 \mu\text{m}$, $3 - 20 \times 20 \mu\text{m}$. The inset presents histograms of the distribution obtained with a constant size ($10 \times 10 \mu\text{m}$) of the region and different resolutions: $I' - 512 \times 512$ pixels, $2' - 256 \times 256$ pixels, $3' - 128 \times 128$ pixels.

Fractal Analysis software package of the NTEGRA SPEC-TRA atomic force microscope, which was produced by NT-MDT, and the Corel DRAW Graphics Suite X8 vector graphics editor were used to determine these parameters. The values of parameters η , ξ , and D_f were found by

counting the closed contours (see the lower inset in Fig. 2, *a*) obtained after tracing the surface irregularities (see the upper inset in Fig. 2, *a*). Varying measurement scale l by a factor of ξ in this fashion, we obtained η contours inscribed into each other that satisfied the topological mixing rule:

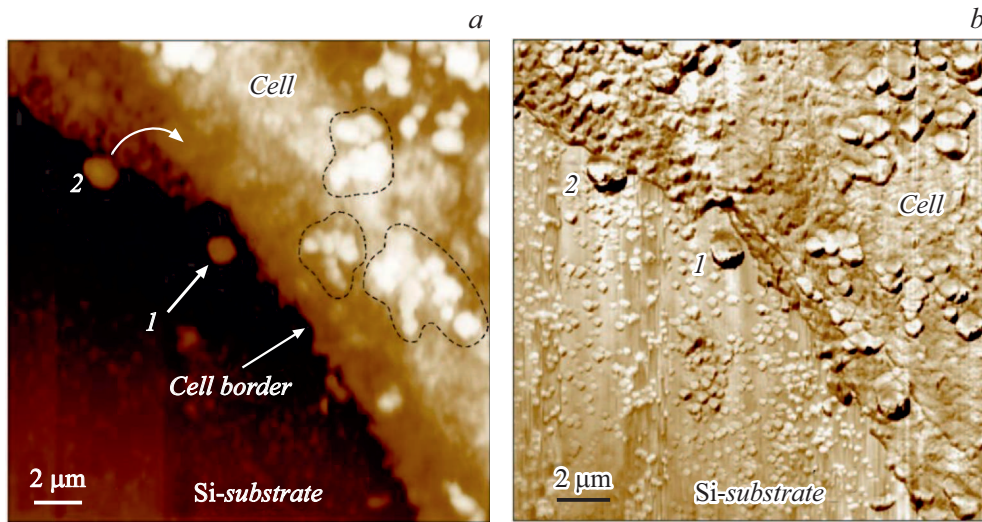


Figure 3. AFM images of the region ($20 \times 20 \mu\text{m}$) of the border surface of a human buccal epithelium cell positioned on a silicon substrate with micro- and nanoparticles adsorbed on it (a) and its phase contrast (b).

these contours did not intersect (see the lower inset in Fig. 2, a).

$$S_{c(fact)} = S_{c(x,y)} \left[\frac{l_i}{l_0} \right]^{D_f - D_T}, \quad l_f = l_{cx} \left[\frac{l_i}{l_0} \right]^{D_f - D_T}. \quad (1)$$

According to the obtained results, surface membrane of human buccal epithelium cell is not smooth and features a rather well-developed Brownian relief $h(x, y)$ formed by randomly spaced folds, protrusions, and other irregularities with a vertical size up to 500 nm. The results of statistical analysis revealed a nontrivial dependence of mean values of surface irregularities $h(x, y)$ on the measurement method (the viewpoint of the external observer; see Fig. 2, b). Histograms of the distribution of surface irregularities $N = N(h)$ (mean value of $\langle h \rangle$ and dispersion σ — root-mean-square deviation $\sqrt{\sigma^2}$ (standard deviation)) depend in this case not only on measurement scale l , but also on the method used to obtain it.

Specifically, the values of these parameters increase (Fig. 2, b, histograms 1–3) as linear measurement scale l increases due to a change in the linear dimensions of the square region (from 5×5 to $20 \times 20 \mu\text{m}$) at a constant resolution of 256×256 dots (pixels). The parameter values grow somewhat less significantly if l increases due to a reduction in the number of scanning dots (pixels), which goes from 512 to 128 at constant linear dimensions $10 \times 10 \mu\text{m}$ (Fig. 2, b, histograms 1'–3'). It is worth reminding that changes in the measurement scale in the global approximation (classical case) translate into dispersion changes, while mean values remain the same. Thus, the strong dependence on the initial conditions (cell condition and sample preparation procedure), the dependence of values of the system parameters on the viewpoint of the external observer (scale l), and the topological mixing property are the necessary and sufficient criteria for classification

of the membrane relief of buccal epithelium cells as a chaotic system. The mathematical framework of fractal geometry is presently used successfully to characterize such systems [12].

Using relations (1) between the geometric parameters of the cell membrane surface and its scaling coefficients and the fractal dimension, one may determine $S_{c(fact)}$ and l_f . Specifically, it follows from (1) that particles $\geq 5 \mu\text{m}$ in size ignore the surface irregularities of the studied cell membrane and travel along it in a linear trajectory with $D_f = D_T = 1$ and length $l_f = l_{cx} \approx 68.6 \mu\text{m}$, which is almost coincident with the projection of the profile of relief section l_{cx} to base $(0;x)$ (Fig. 1, b, trajectory 1). The point with $D_f = 2$, which corresponds to $l \approx 200 \text{ nm}$ (Fig. 1, b, trajectory 2), is an important point on the $D_f = D_f(l)$ dependence. Particles with this size perceive the membrane relief as a two-dimensional surface with $D_f = 2$ ($l_i = 68.6 \mu\text{m}$, $l_0 = 0.2 \mu\text{m}$, $D_T = 1$) and need to travel an average distance of $l_f \approx 23\,530 \mu\text{m}$ to traverse it. Particles smaller than $\sim 200 \text{ nm}$ are sensitive to almost all surface irregularities and move along the membrane as a three-dimensional fractal surface with $D_f > 2$. As a result, their travel path is significantly longer. For example, this path length for a particle with size $l \leq 100 \text{ nm}$ $D_f = 2.40$ ($l_i = 68.6 \mu\text{m}$, $l_0 = 0.1 \mu\text{m}$, $D_T = 1$) may exceed $l_f > 641\,472 \mu\text{m}$ (Fig. 1, b, trajectory 3). According to (1), the actual area of the upper surface of the studied cell membrane is more than 13.6 times higher than the area of its projection $S_{c(x,y)} \approx 4848.33 \mu\text{m}^2$, and at $l = 0.1 \mu\text{m}$ ($l_i = 68.6 \mu\text{m}$, $D_T = 2$, $D_f = 2.40$) it assumes a value of $S_{c(fact)} \approx 66\,088 \mu\text{m}^2$.

The results of experimental studies of the processes of particle motion along the cell membrane surface verify these conclusions. Figure 3 presents the image of the border of a human buccal epithelium cell adjacent to the surface of a silicon substrate containing a large number

of adsorbed micro- ($< 2 \mu\text{m}$) and nanoparticles ($> 30 \text{ nm}$). The observed micro- and nanoparticles formed on the silicon substrate as the buffer solution dried out. The examination of the phase composition revealed that the membrane surface was free from such particles. Apparently, this was attributable to the fact that the membrane was protected by the buffer solution layer.

It follows from Fig. 3 that the largest ($> 1 \mu\text{m}$) particles (e.g., particles 1 and 2 in Fig. 3, *a*) reach the cell surface first and start moving along it. This is evidenced by the increased concentration of such particles on the membrane surface (the gradient of concentration relative to the silicon substrate). At the same time, particles larger than one micrometer are almost lacking on the substrate surface (the only exceptions are particles 1 and 2 in Fig. 3, *a*): all of them are positioned on the membrane surface and had already formed fairly large agglomerations there (see the regions enclosed by dashed curves in Fig. 3). These conclusions agree well with the phase contrast image: almost all nanoparticles smaller than 400 nm remain on the silicon substrate surface, and almost all larger particles are positioned on the cell membrane (Fig. 3, *b*). Specifically, while particle 1 $\sim 1 \mu\text{m}$ in size approaches the membrane surface, another (similar) particle 2 has already reached this surface.

Funding

This study was supported financially by the Sevastopol State University (project identifier 42-01-09/90/2020-1).

Compliance with ethical standards

All procedures performed in studies involving human participants were in accordance with the ethical standards of the institutional and/or national research committee and with the 1964 Helsinki Declaration and its later amendments or comparable ethical standards. Studies involving the collection of buccal epithelium were approved by the Ethics Committee of the Sevastopol State University (study No. 3; July 15 2021). Buccal epithelium was collected in accordance with the code of conduct for research on human materials in the Russian Federation. Informed voluntary consent was obtained from all participants involved in the study.

Conflict of interest

The authors declare that they have no conflict of interest.

References

- [1] A.S. Shanbhag, J.J. Jacobs, J. Black, J.O. Galante, T.T. Glant, *Clin. Orthop. Rel. Res.*, **342**, 205 (1997).
- [2] A. Poliakov, V. Pakhaliuk, V.L. Popov, *Front. Mech. Eng.*, **6** (4), 16 (2020). DOI: 10.3389/fmech.2020.00004
- [3] E.N. Aybeke, S. Ployon, M. Brulé, B. De Fonseca, E. Bourillot, M. Morzel, E. Lesniewska, F. Canon, *Langmuir*, **35** (39), 12647 (2019). DOI: 10.1021/acs.langmuir.9b01979
- [4] N.N. Belyaeva, L.P. Sycheva, V.S. Zhurkov, *Otsenka tsitologicheskogo i tsitogeneticheskogo statusa slizistykh obolochek polosti nosa i rta u cheloveka: metodicheskie rekomendatsii* (M., 2005) (in Russian).
- [5] A.G. Proshin, N.A. Durnova, V.N. Sal'nikov, M.N. Kurchatova, N.V. Sal'nikov, *Vestn. REAVIZ*, №. 1(37), 74 (2019) (in Russian).
- [6] A. Kubiak, T. Zieliński, J. Pabijan, M. Lekka, *Int. J. Mol. Sci.*, **21** (22), 8786 (2020). DOI: 10.3390/ijms21228786
- [7] M.A. Pal'tsev, I.M. Kvetnoi, V.O. Polyakova, S.S. Konovalov, O.M. Litvyakova, N.S. Lin'kova, H.H. Sevost'yanova, A.O. Durnova, G.Kh. Tolibova, *Mol. Med.*, №. 4, 18 (2012) (in Russian).
- [8] H. Tejada-Mora, L. Stevens, M. Gröllers, A. Katan, E. van de Steeg, M. van der Heiden, *Biophys. J.* (Posted September 10, 2019). DOI: 10.1101/761627
- [9] A.A. Wagh, E. Roan, K.E. Chapman, L.P. Desai, D.A. Rendon, E.C. Eckstein, C.M. Waters, *Am. J. Physiol. Lung Cell. Mol. Physiol.*, **295** (1), L54 (2008). DOI: 10.1152/ajplung.00475.2007
- [10] R.G. Bailey, R.D. Turner, N. Mullin, N. Clarke, S.J. Foster, J.K. Hobbs, *Biophys. J.*, **107** (11), 2538 (2014). DOI: 10.1016/j.bpj.2014.10.036
- [11] M. Lasalvia, S. Castellani, P. D'Antonio, G. Perna, A. Carbone, A.L. Colia, A.B. Maffione, V. Capozzi, M. Conese, *Exp. Cell Res.*, **348** (1), 46 (2016). DOI: 10.1016/j.yexcr.2016.08.025
- [12] J. Feder, *Fractals* (Springer, New York, 1988).